Vibrational dephasing in molecular mixed crystals: a picosecond time domain CARS study of pentacene in naphthalene and benzoic acid

Koos Duppen, D. P. Weitekamp, and Douwe A. Wiersma

Picosecond Laser and Spectroscopy Laboratory, Department of Physical Chemistry, University of Groningen, Nijenborgh 16, 9747 AG Groningen, The Netherlands
(Received 1 June 1983; accepted 31 August 1983)

Multiresonant time-domain coherent anti-Stokes Raman scattering (CARS) experiments have been employed in a study of the decay of vibrational coherences of pentacene doped into naphthalene and benzoic acid. In all cases, the CARS decay is found to be exponential, which indicates that the electronic and vibronic inhomogeneities in this system are strongly correlated. The temperature dependence of vibrational dephasing shows no effect of coupling to the lowest-frequency librational mode of pentacene that is known to dominate electronic dephasing. This surprising result can be understood on basis of a dephasing model where rapid coherence exchange exists between a cold vibrational transition and a corresponding near-resonant librationally hot one. For the 767 cm^{-1} vibrational transition, oscillations of the CARS signal as a function of delay are shown to arise from interference at the detector with a nearby naphthalene host signal. An inconsistency with a previously reported spontaneous Raman study is resolved by showing that the signal observed there is actually site-selected fluorescence.

I. INTRODUCTION

A. Vibrational relaxation of polyatomic molecules in the solid state

Remarkably little is known about the vibrational relaxation and dephasing of organic molecules in the solid state. Much work has focused on relaxation within the first excited singlet manifold S_1, since it is accessible by optical absorption,[1,2] unrelaxed fluorescence,[3–6] photon echo,[7,8] and hole burning[9–11] studies. On the other hand, the ground state manifold is conceptually simpler territory for vibrational studies, since here one is free of the competing phenomena of electronic relaxation and dephasing and the complications of multiple potential energy surfaces. The methods that have been applied to organic solid state studies of ground state relaxation are spontaneous Raman scattering,[12–19] infrared spectroscopy,[17,20,21] both frequency,[22–24] and time domain[25–28] four wave mixing, and, recently, vibrational grating diffraction.[30]

For molecules with more than a few atoms, the overall picture which emerges is that in the lowest temperature range the vibrational linewidth or the dephasing time $T_2 < 2\times10^2$ ps is constant, but that a thermally activated dephasing sets in at < 50 K. In the usual two level picture the total rate of dephasing or irreversible transverse relaxation can be written as

$$1/T_2 = 1/T_2^* + 1/2T_1 , \qquad (1)$$

where $1/T_1$ is the population relaxation rate and $1/T_2^*$ is the pure dephasing rate. The latter is theoretically zero in the limit $T \to 0$[31] and the equivalence $T_2 = 2T_1$ at low temperature was demonstrated experimentally for an excited state vibration using two pulse and three pulse photon echoes.[7]

The full experimental characterization of the temperature dependence would require separate experiments for T_2 and T_1 allowing a separation of the pure dephasing and population contributions to Eq. (1). In the absence of such data, the practice has been to use theoretical models for the temperature dependence of each contribution to decide between these contributions. In this way it is deduced that the spontaneous Raman linewidths for ground state phonons in *p*-bromochlorobenzene and *p*-dichlorobenzene[17] and the linewidths[15] and coherence decays[26] for phonons in naphthalene are lifetime limited, not only at the lowest temperature, but also over some range of the thermal activation. On the other hand for higher frequency modes, corresponding to internal vibrations of the isolated molecule, the temperature dependence has been attributed to T_2 processes in which the thermal activation of the low frequency modes randomly modulates the observed frequency through common cubic and quartic anharmonic terms.[1,2,12–14,16,18,19,24]

B. Pentacene as guest in mixed molecular crystals

Because of its large $S_1 \leftarrow S_0$ oscillator strength, convenient transition frequency and relatively simple structure, pentacene is a model compound for large molecule relaxation studies. It can be doped into a number of molecular crystals and its electronic and vibronic dephasing in these systems have been extensively studied, primarily with photon echo techniques.[7,8,32] With reference to the energy level diagram of Fig. 1(a), these studies have shown that the temperature dependent dephasing of the $S_1 \leftarrow S_0$ origin ω_{ca} and various vibronic transitions ω_{da} is due to the independent scattering in the ground and excited manifolds[33] to local phonon states (indicated by primed kets and dotted lines), which lie ~ 15 cm^{-1} above each of the unprimed phononless states. This local phonon mode corresponds to a torsional libration of the molecular plane in the intermolecular site potential.[7] At temperatures where $kT \gtrsim h\omega_{ll'}$, states with several quanta in the local mode progression (not shown) will become significantly occupied along with the

 0021-9606/83/245835-10$02.10

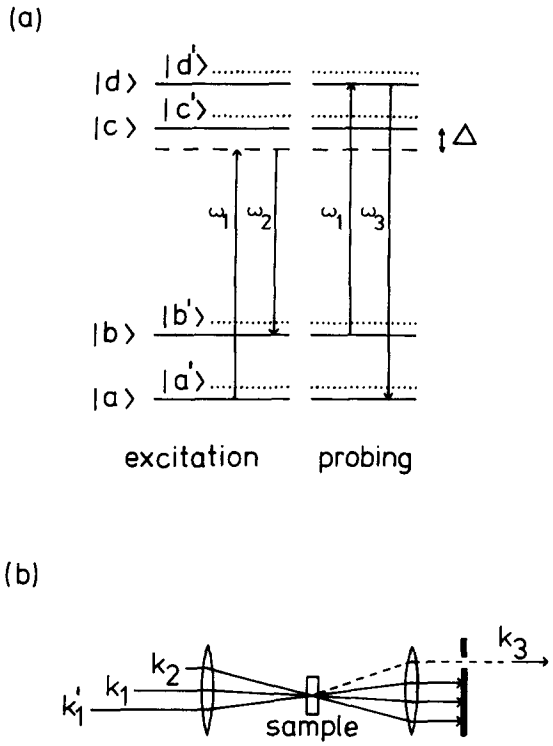

FIG. 1. Level diagram and phasematching for the time-domain CARS process. (a) Coherence is prepared between ground state $|a\rangle$ and vibrationally excited state $|b\rangle$ by simultaneous pulses at ω_1 and ω_2. After a delay t_1 indicated by a break in the center, the coherence is probed by another pulse at frequency ω_1. This process is exactly resonant through the level $|d\rangle$, which is the corresponding vibrational state in the electronically excited S_1 manifold. The parameter Δ is the detuning of ω_1 and ω_2 from ω_{ca} ($S_1 \leftarrow S_0$) and ω_{cb}, respectively. The primed levels are libirational (local phonon) states about 15 cm^{-1} above the unprimed phononless states. (b) Spatial filtering is used in the detection to separate the delayed signal from other (two pulse) CARS signals. The desired three-pulse signal has wave vector $\mathbf{k}_3 = \mathbf{k}_1 + \mathbf{k}_1' - \mathbf{k}_2$. Subsequent frequency filtering by a monochromator is not shown.

single phonon states $|i'\rangle$.

Studies of the ground state vibrational dephasing of pentacene have been reported in two host crystals. In benzoic acid the 756 cm^{-1} mode was observed by frequency domain coherent Stokes Raman scattering (CSRS) from 4.2 to 200 K and found to broaden exponentially with an activation energy of $\Delta E/hc = 97$ cm^{-1}.[24(a)] The low temperature T_2 of 24 ps found in this study is contradicted by time domain coherent anti-Stokes Raman scattering (CARS), as reported previously[28,29] and also by the frequency domain CARS.[24(c)] In Sec. IID we return to this point and present temperature dependent data obtained with time domain CARS. For the system pentacene in naphthalene a reported resonance-enhanced spontaneous Raman study found an exponential activation of the linewidth of the 756 and 994 cm^{-1} modes with $\Delta E/hc = 17$ cm^{-1}.[34] This was interpreted as implicating the local mode in the vibrational dephasing. In Appendix A we show that in fact the signals observed in that study were fluorescence and we explain how the observed linewidths and laser-dependent line positions arise from site selection in conjunction with the well-known electronic dephasing. The actual temperature dependence of the vibrational dephasing of the 756 cm^{-1} pentacene mode in naphthalene obtained by delayed CARS is presented in Sec. IID.

C. Time domain CARS

The transitions indicated by arrows in Fig. 1(a) are those involved in the coherent nonlinear spectroscopic technique of time domain (or delayed) coherent anti-Stokes Raman scattering (CARS). Extensive references to the method may be found in Ref. 29. The energy level diagram of Fig. 1(a) is split vertically to indicate the two time periods in the experiment in which the system interacts with the radiation. In the excitation or preparation period indicated on the left-hand side, simultaneous pulses at optical frequencies $\omega_1 = \omega_{ca} - \Delta$ and $\omega_2 = \omega_{cb} - \Delta$ cross in the sample with wave vectors $\mathbf{k}_1$ and $\mathbf{k}_2$. The difference frequency $\omega_1 - \omega_2 = \omega_{ba}$ is thus resonant with a ground state vibrational transition and prepares a coherent superposition of states $|a\rangle$ and $|b\rangle$. The delay or evolution period of variable length t_1 follows, after which a probe pulse of frequency ω_1 and wave vector $\mathbf{k}_{1'}$, crosses the excited volume. As drawn, ω_1 is exactly resonant with a dipole allowed transition between the ground state vibrational state $|b\rangle$ and an analogous state $|d\rangle$ in the excited manifold. This results in the stimulated emission at $\omega_3 = 2\omega_1 - \omega_2$ being at ω_{da}, as in the figure. As sketched in Fig. 1(b) the direction of this emission is $\mathbf{k}_3 = \mathbf{k}_1 + \mathbf{k}_{1'} - \mathbf{k}_2$, which allows spatial filtering as well as frequency filtering (not shown) of the signal. The amplitude of this emitted field is proportional to the amplitude of the vibrational coherence between $|a\rangle$ and $|b\rangle$ which remains at the time of the probe pulse.

An extensive discussion of this delayed CARS experiment in these systems is given elsewhere.[29] There the principal goal was the development and demonstration of a formalism for the calculation of the dependence of the signals on the pulses to all powers of the applied fields. The use of intense pulses is motivated by the desire to excite over a range of vibrational and electronic frequencies, while taking maximum advantage of the signal enhancement possible near electronic resonance. Experimental aspects treated were optimization of the probe pulse energy and the role of free induction decay at ω_{da} in the observed signal.

For the present purpose of studying vibrational dephasing it is only necessary to realize that with all pulse intensities fixed the CARS signal intensity decays as $\exp(-2t_1/T_2)$ where $T_2 \equiv T_2^{ab}$ is the transverse decay time for the two level subspace consisting of $|a\rangle$ and $|b\rangle$. By varying ω_1 and ω_2 the identities of the states labeled $|b\rangle$ and $|d\rangle$ are changed and different modes are studied.

II. RESULTS AND DISCUSSION

A. Experimental

Pentacene (Fluka) was used without purification and added to zone refined naphthalene or benzoic acid. Crystals were grown by the Bridgman method with a

final concentration of 10^{-5} M/M. These were cut along the a–b cleavage plane to a thickness of 0.4 to 1.0 mm and mounted in a variable temperature He cryostat. The light polarization was along the b axis of the naphthalene crystals and the a axis of the benzoic acid crystals.

The system of pentacene in benzoic acid is known to undergo, with low quantum yields, a number of photon induced site rearrangements which lead to spectroscopically distinct environments for the pentacene guest.[35–37] These processes have no apparent effect on the delayed CARS signals; the scans were reproducible and showed no measurable change with time at fixed delay.

The light source is two synchronously pumped dye lasers with Rh 6G and Rh B used for the frequencies ω_1 and ω_2, respectively. These pulses were amplified in two-stage dye cell amplifiers pumped at 10 Hz by the second harmonic of a Nd–YAG laser. The amplifiers contained Rh 6G for ω_1 and Rh B for ω_2 in the case of pentacene in benzoic acid and Rh B and Rh 101, respectively, when pentacene in naphthalene was studied.

For all delayed CARS experiments the pulses at ω_1 and ω_2 have an intensity FWHM of 6 ps. For the frequency domain CARS measurements and for fluorescence line narrowing experiments this was increased to 85 ps by inserting in each cavity a high free spectral range etalon (Spectra Physics) and a 3 mm quartz plate. Additional details and a diagram of the experimental arrangement may be found in Ref. 29.

B. Frequency dependence of the signals

While the information on vibrational dephasing is from time domain CARS experiments, it is first necessary to demonstrate that the signals do in fact arise from the guest resonances of interest. To this end the CARS signals arising from coincident ω_1 and ω_2 pulses were studied as a function of the frequencies ω_1 and ω_2. The laser linewidth is transform limited to ~0.2 cm^{-1}.

Figure 2 shows such an experiment on the system pentacene in benzoic acid at two different power levels. The frequencies ω_1 and ω_2 were changed together at a fixed difference of $(\omega_1 - \omega_2)/2\pi c = 756$ cm^{-1} corresponding to a ground state fundamental of pentacene which is prominent in the fluorescence spectrum.[22] A single resonance is observed at $2\pi c/\omega_1 = 5884.8$ Å. This corresponds to $\omega_1 = \omega_{db}$ of Fig. 1(a) and is a resonance predicted both in the $\chi^{(3)}$ formalism[22,38] and in the nonperturbative approach.[29]

The ~1 cm^{-1} width of this resonance at low power (0.2 μJ/pulse at ω_1 and ω_2, solid curve in Fig. 2) is consistent with the inhomogeneous width of the ω_{db} electronic transition which must be similar to that of the ω_{da} or ω_{cb} transitions [Fig. 1(a)] observable in absorption and fluorescence, respectively.

At high power (2.0 μJ/pulse at ω_1 and ω_2) the resonance broadens to ~8 cm^{-1} (dashed curve of Fig. 2). This can be qualitatively explained as power broadening on the ω_{db} transition. The results of probe pulse saturation studies in the delayed experiment[29] show that the Rabi frequency at beam center for this transition, pulse length, and pulse energy is ~6 cm^{-1}.

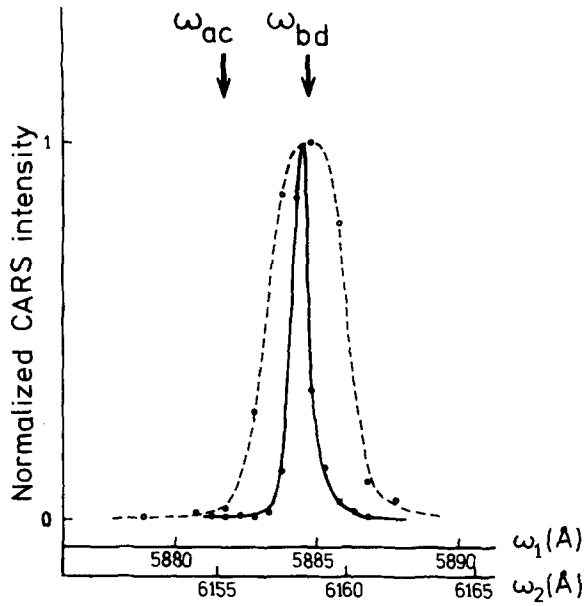

FIG. 2. Normalized CARS intensity in a two-pulse frequency domain experiment on pentacene in benzoic acid. The frequency of both lasers is changed simultaneously with a fixed energy difference of 756 cm^{-1}. The two possible electronic resonance enhancements are indicated by arrows. The solid curve is obtained with low laser power (0.2 μJ/pulse). At ten times greate energy (dashed curve) power broadening is evident.

A second resonance is possible at $\omega_1 = \omega_{ca}$. This signal must be at least three orders of magnitude smaller under the present conditions, since it is not visible in Fig. 2. While a quantitative explanation for this is lacking, it should be noted that the absorption of ω_1 at this frequency is nearly complete. Thus the CARS generation is not uniform over the path of the beams through the crystal, as is the case when $\omega_1 = \omega_{db}$. Attempts to repeat this experiment on lower concentration crystals (4×10^{-7} M/M) were unsuccessful; neither resonance is seen. This illustrates the quadratic dependence of these coherent signals on number density. It is possible that at some intermediate concentration the missing resonance would be seen.

Identical results to those in Fig. 2 were found for pentacene in naphthalene, except that in this host $2\pi c/\omega_{db} = 6030.9$ Å. In addition, in this host the vibrational resonance was demonstrated by varying ω_2 with ω_1 fixed at ω_{db}. Another confirmation of the identity of the delayed signal is the agreement of the low temperature decay with the narrowed spontaneous emission linewidth at ω_{cb}. This is discussed in Appendix A.

C. Low temperature dephasing

Figure 3 shows a typical decay as a function of the probe pulse delay t_1 for the time domain CARS experiment. The transition is the 756 cm^{-1} vibration of pentacene in naphthalene at 4.2 K. The preparation pulse

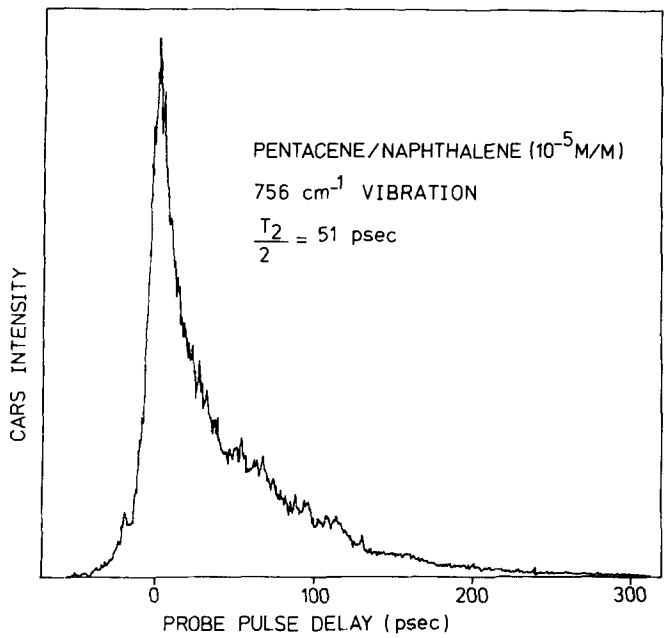

FIG. 3. Time domain CARS intensity as a function of the probe pulse delay for the 756 cm^{-1} vibration of pentacene in naphthalene at 4.2 K.

energies are 25 nJ at ω_1 and 30 nJ at ω_2. The probe pulse energy is 35 nJ. Note that the noise level decreases with the signal level. This is an indication that the noise is dominated by instabilities from shot to shot. After an initial period on the order of the pulse cross correlation the decay is exponential.

This is more readily seen in the logarithmic plot of Fig. 4. The lower curve is the same data as in Fig. 3. The middle and upper curves are the same experiment with the energy of all pulses increased by a factor of 10 and 100, respectively. Perturbation theory predicts an increase by 10^3 between the successive curves (linearity in each of the three applied pulses). The observed increases are far less in both the delayed signal and the $t_1 \simeq 0$ signal. The latter signal, which is present only in the region of pulse overlap, may have contributions from the host.[25,27,29] The saturation of the delayed signal is largely due to the probe process and this has been studied in detail.[29]

Comparison of the three curves shows that there is no measurable dependence of the decay time $T_2/2 = 51 \pm 3$ ps on pulse power. This illustrates a fundamental advantage of time domain experiments: they measure the free evolution of the system in the absence of applied fields.

The logarithmic plots for several pentacene vibrations in the benzoic acid host are shown in Fig. 5. The lowest curve in Fig. 5 is for the 260 cm^{-1} vibration and the 5.5 ps decay is dominated by the cross correlation of the pulses. This indicates the time resolution of the experiment, which has contributions from both the pulse length and from timing jitter between ω_1 and ω_2.

Table I summarizes the low temperature results for the different vibrations observed in the two hosts. For

TABLE I. Low-temperature dephasing times for various ground manifold pentacene vibrations ω_{ba} in two host crystals. Frequencies are in cm^{-1}. Also listed are the corresponding excited state frequencies ω_{dc} and the laser offsets Δ used as in the scheme of Fig. 1(a).

Host	$\omega_{ba}/2\pi c$	$\omega_{dc}/2\pi c$	$\Delta/2\pi c$	T_2 (ps)
Benzoic acid	260	258	2	6
Benzoic acid	355	339	16	34
Benzoic acid	501	490	11	45
Benzoic acid	603	598	5	53
Benzoic acid	756	747	9	70
Benzoic acid	763	761	2	18
Benzoic acid	789	791	−2	59
Naphthalene	756	747	9	101
Naphthalene	767	763	4	120

each experiment it was possible to observe the vibronic transitions at ω_{da} and ω_{cb} in absorption and fluorescence respectively and thus to choose the frequencies of ω_1 and ω_2 according to the scheme of Fig. 1(a). In all cases the decay was measured over two to three decades after the initial nonexponential region of pulse overlap and found to be exponential. This suggests that inhomogeneity of the vibrational frequencies is negligible. This is not unexpected; if the fractional inhomogeneity of a vibrational frequency is the same as for an electronic transition in these systems (~1 cm^{-1}/1.6 $\times 10^4$ cm^{-1}), then its contribution is unobservably small on the time scale of the exponential T_2.

As discussed in connection with Eq. (1), these values for the low temperature limits of the vibrational T_2 are expected to be 2 T_1. More specifically, since the lower

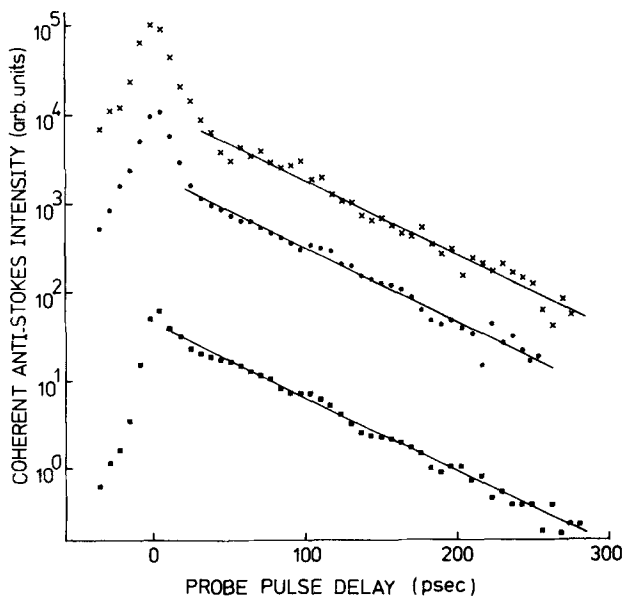

FIG. 4. Logarithmic plot of the CARS intensity as a function of the probe pulse delay for the 756 cm^{-1} vibration of pentacene in naphthalene at 4.2 K. The lower trace (■) is the decay of Fig. 3, which is taken at pulse energies of 30 nJ. In the curves above all the pulse intensities have been increased by a factor of 10 (○) and 100 (×), respectively.

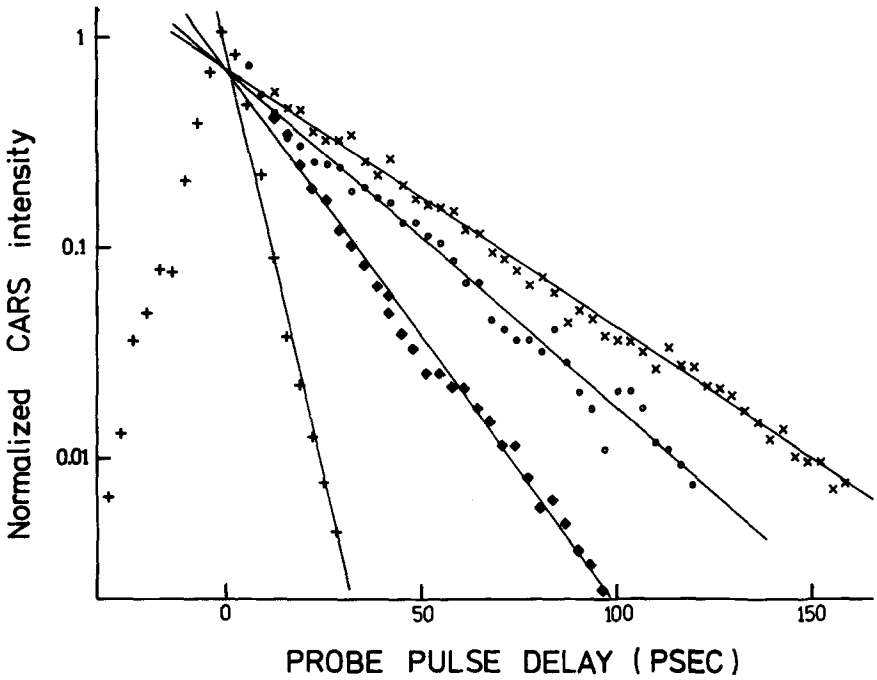

FIG. 5. Logarithmic plot of the CARS decay for different vibrations of pentacene in benzoic acid. The intensities are normalized to one at zero delay. From top to to bottom, the four lines are fits to the exponential decays for the vibrations at 756 cm^{-1} (×, $T_2 = 70$ ps), 603 cm^{-1} (○, $T_2 = 53$ ps), 355 cm^{-1} (◆, $T_2 = 34$ ps) and 260 cm^{-1} (+). This last decay is dominated by the cross correlation of the pulses, which is largely due to the timing jitter between the ω_1 and ω_2 pulses.

state $|a\rangle$ of the transition is always the stable ground state, $(T_1)^{-1}$ is the rate out of $|b\rangle$. Even from the limited data of Table I it is evident that there is no simple systematic dependence of the low temperature population relaxation on vibrational energy in this spectral region. The same conclusion was drawn for the excited state vibrations of pentacene[8] and porphins[10,11] on the basis of photon echo and hole burning studies at low temperature. The host dependence of the dephasing times also suggests that any understanding will have to include a model of the differences in intermolecular interactions. On the other hand, it would be premature to assume that the vibrational energy of the guest is directly delocalized into host degrees of freedom. The possible role of lower guest modes as intermediates in the radiationless decay route is a subject of continuing research.

D. Temperature dependence of the vibrational dephasing

As mentioned in Sec. IB, an important motivation for the present study is the question of the role of the local phonon in the vibrational relaxation. In the lower curve of Fig. 6, the linewidth of the $\omega_{ba}/2\pi c = 756$ cm^{-1} mode of pentacene in naphthalene is plotted as a function of temperature. This linewidth is $(\pi c T_2)^{-1}$, with T_2 determined by the time domain CARS experiment. For comparison, the upper curve is the analogous homogeneous linewidth for the vibronic transition ω_{da} determined by Hesselink and Wiersma[7] with two pulse photon echoes. For this *vibronic* dephasing Eq. (1) applies again with T_1 being the lifetime of the excited state vibration [$|d\rangle$ in Fig. 1(a)] and T_2^* given by the optical-Redfield theory of De Bree and Wiersma[33] as

$$1/T_2^* = \tfrac{1}{2}[\tau_{a'}^{-1} \exp(-h\omega_{a'a}/kT) + \tau_{d'}^{-1} \exp(-h\omega_{d'd}/kT)] . \quad (2)$$

Here $\tau_{a'}$ and $\tau_{d'}$ are the spontaneous decay rates from $|a'\rangle$ to $|a\rangle$ and $|d'\rangle$ to $|d\rangle$, respectively. Equation (2) incorporates the assumption of independent scattering of the local phonon in the ground and excited states and generally the ground and excited state parameters differ.[7,33]

Evidently, the *vibrational* dephasing is insensitive to the thermal activation of local phonon scattering, becoming only slightly more rapid over the temperature

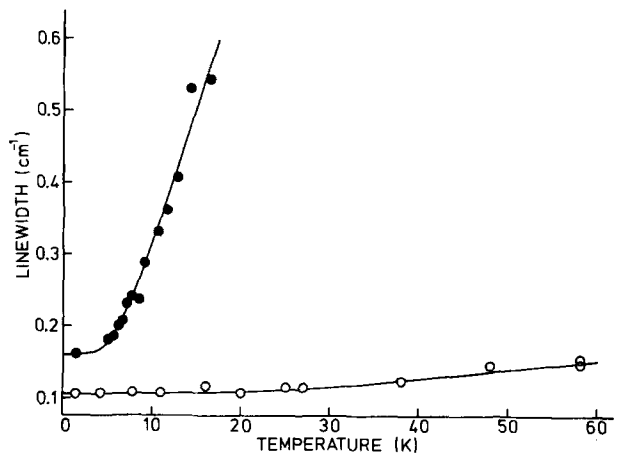

FIG. 6. Temperature dependence of the linewidth of the 756 cm^{-1} vibrational transition (ω_{ba}) of pentacene in naphthalene as determined by time resolved CARS (open circles, lower trace) and of the 747 cm^{-1} vibronic transition (ω_{da}) as determined by two pulse photon echoes (Ref. 7) (closed circles, upper trace). The solid lines are fits to Eq. (4) with $\Delta E/hc = 60$ cm^{-1} and $T_2^*(\infty) = 55$ ps for the ground state vibration and $\Delta E/hc = 17$ cm^{-1} and $T_2^*(\infty) = 6$ ps for the vibronic transition. The latter values represent a two parameter approximation to Eq. (3). See Ref. 7.

range where the Bose–Einstein thermal average local phonon occupation number $[\exp(h\omega_{i'i}/kT)-1]^{-1}$ ranges from $\sim 10^{-7}$ to ~ 1.8. A form analogous to Eq. (2) with $|b\rangle$ as the final state is not consistent with the data. Thus independent phonon scattering in $|a\rangle$ and $|b\rangle$ is ruled out. One way in which the effect of the local phonon could be attenuated is if the phonon scattering in $|a\rangle$ and $|b\rangle$ is *correlated* and if the change in vibrational frequency $\delta \equiv \omega_{b'a'} - \omega_{ba}$ is sufficiently small that rapid frequency averaging occurs on the time scale of T_2. This is the limit of fast exchange[12–14,33] and leads to the temperature dependent pure dephasing contribution

$$1/T_2^* = \delta^2 \tau_{ph} \exp(-h\bar{\omega}/kT)(1+\delta^2\tau_{ph}^2)\,, \tag{3}$$

where $\bar{\omega} = \frac{1}{2}(\omega_{b'b} + \omega_{a'a'})$ is the average phonon frequency and τ_{ph} is the decay rate of $|b'\rangle$ into $|b\rangle$ or $|a'\rangle$ into $|a\rangle$, which are necessarily identical in this model. The preexponential factor here is to a good approximation $\delta^2\tau_{ph}$, which is a factor of $(\delta\tau_{ph})^2$ smaller than for the case of uncorrelated scattering appropriate to electronic and vibronic dephasing [Eq. (2)].

With the values of $\tau_{ph} = 3.5$ ps and $\bar{\omega}/2\pi c = 18$ cm^{-1} taken from the electronic dephasing studies[7] and with T_1 assumed to be constant, no satisfactory fit was possible with Eq. (3) to the CARS data on Fig. 6 for any δ. The situation is similar in the benzoic acid host (Fig. 7), where T_2 has a greater variation over the available temperature range. No fit with an activation parameter near the local phonon frequency $\bar{\omega}/2\pi c \lesssim 16$ cm^{-1} [36,39,40] was possible with any preexponential factor. Thus the thermal activation of the vibrational T_2 at the local phonon energy is negligible. Since the phonon is known to be present, the system is undergoing fast exchange in the sense that δ is less than the low temperature vibrational linewidth.

The equality of the phonon energies and lifetimes deduced here for different states of the ground state manifold is consistent with the similar conclusion for the S_1 manifold made on the basis of temperature dependent photon echo studies at different vibronic frequencies.[7,8] However, the present ground state results establish these equalities more directly and with far narrower limits. Comparable results in the excited manifold should be possible with delayed CSRS.[29] It appears though that within either manifold separately the local phonon is to a good approximation a separable degree of freedom.

Evidently another mechanism is needed to explain the reduction of T_2 with temperature and this must involve higher energy excitations to be consistent with the extended region of nearly constant T_2 at the lowest temperatures. A more general form than Eq. (3) is the Arrhenius form:

$$1/T_2^* = [1/T_2^*(\infty)]\exp(-\Delta E/kT) \tag{4}$$

with arbitrary parameters $T_2^*(\infty)$ and ΔE. Such a fit could point to some other low frequency mode of energy ΔE acting either within an exchange model [Eq. (3)] or the more general dynamic coupling model.[41] It could also point to the interaction of the observed fundamental at 756 cm^{-1} with another nearby fundamental through quartic off diagonal terms involving a mode of energy ΔE.[42]

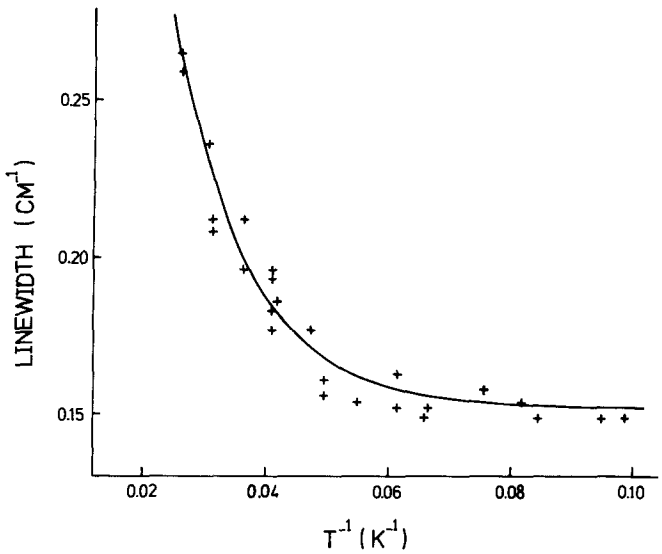

FIG. 7. Temperature dependence of the linewidth of the 756 cm^{-1} vibrational transition of pentacene in benzoic acid. The fitted curve is of the form of Eq. (4) with $\Delta E/hc = 65$ cm^{-1} and $T_2^*(\infty) = 8$ ps.

The results of fitting to Eq. (4) are, for the naphthalene host (Fig. 6), $T_2^*(\infty) = 55^{+45}_{-25}$ ps and $\Delta E/hc = 60 \pm 25$ cm^{-1}. For the benzoic acid host (Fig. 7) the corresponding parameters are $T_2^* = 8^{+7}_{-3}$ ps and $\Delta E/hc \pm 15$ cm^{-1}. The error ranges for the two parameters are correlated; the high range of $T_2^*(\infty)$ being associated with the low range of $\Delta E/hc$. The large uncertainty for the napthalene host is due to the small temperature dependence in that system.

The fit in the benzoic acid system is more definite and in addition for this system comparison can be made with results obtained with frequency domain four wave mixing on the same 756 cm^{-1} ground state transition.[24(a)–24(c)] Using a CSRS arrangement with $\omega_1 = \omega_{ca}$ and ω_2 tuned near ω_{da}, the parameters $T_2^*(\infty) = 1.0$ ps and $\Delta E/hc = 97$ cm^{-1} were found from the temperature dependent width of the resonance at $\omega_2 - \omega_1 = \omega_{ba}$. Note that the activation parameters in the caption of Fig. 3 of Ref. 24(a) should be multiplied by $\log_e x/\log_{10} x = 2.30$ to correct a numerical error[24(b)] and that these then correspond to $1/2\pi c\, T_2^*(\infty)$ in the present context [Eqs. (1) and (4)]. That data set extends to higher temperatures (40–200 K) inaccessible in the present time domain CARS experiments, but shows total linewidths at lower temperatures greater by a factor of 3 than those given in Fig. 7. Recently, the frequency domain CARS experiment has been reported at low temperature.[24(c)] The linewidth with this method is 50% greater than the asymptotic value of Fig. 7. No error limits are cited.

It has been suggested[24(c)] that the failure of the frequency domain CSRS experiment[24(a)] to measure the ground state vibrational T_2 is evidence for the imperfect correlation of the inhomogeneous distributions of the different electronic transitions.

Continuation to higher temperatures of the results obtained here is evidently needed to establish the adequacy of a single exponential form. This is currently impeded by two phenomena. At higher temperatures vibrational dephasing becomes comparable to the time resolution of the apparatus, which is limited to ~6 ps by a combination of pulse width and timing jitter between the ω_1 and ω_2 pulses. The time resolution problem is exacerbated by a decline in signal size at higher temperatures. As we know from the temperature dependent electronic and vibronic dephasing studies, these transverse relaxation times become shorter than the time scale of the pulses. This decreases the efficiency of both the preparation and probing processes in this near-resonant regime. Both difficulties would be mitigated by using shorter pulses.

It is interesting that the best fit activation energies found in the two different hosts are similar despite the different preexponential factors. These energies are in the range expected for host librations or a higher energy guest libration. Additional spectroscopic evidence is needed to make a definite assignment of the mode responsible and to rationalize the preexponential factors.

Finally, it should be emphasized that the possibility of a temperature dependent T_1 has been set aside in interpreting the data in terms of Eq. (4). Experiments which independently measure T_1 are possible[30] and should allow this issue to be checked.

E. Guest-host quantum beats

For the majority of the modes studied, it was possible to neglect the host contributions entirely when considering the delayed signal. An exception is the 767 cm^{-1} vibration of pentacene in naphthalene, whose CARS decay is shown in Fig. 8. Pronounced beats are observed in the signal, indicating the presence of two nondegenerate contributions to the decay. The beat period of 34.5 ps indicates a frequency separation of ~1 cm^{-1}. Thus the second component can be assigned to the 766 cm^{-1} vibration of the host, which has already been characterized in a delayed CARS study of pure naphthalene.[25] The reported assignment for these transitions indicates that they are analogous C–C stretch modes in the two different molecules.[43]

The simulation in Fig. 8 is a fit to the form

$$I(t) = \left| a \exp(-t_1/T_2^p) + b \exp(i\phi_b) \exp(-t_1/T_2^n) \right|^2$$

$$= a^2 \exp(-2t_1/T_2^p) + b^2 \exp(-2t_1/T_2^n) + 2ab \cos(\phi_b^0 + \Delta\omega t)$$

$$\times \exp\{-t_1 [(1/T_2^p) + (1/T_2^n)]\} , \quad (5)$$

where the real parameters $a = 0.2$ and $b = 0.8$ are the amplitudes of the two fields interfering at the detector and $\phi_b = \phi_b^0 + \Delta\omega t_1$ is their phase difference, which is time dependent due to the frequency difference $\Delta\omega$. The naphthalene dephasing time $T_2^n = 156$ ps is taken to be identical with that measured in the pure crystal.[25] The pentacene dephasing time of $T_2^p = 120 \pm 10$ ps is a fitting parameter. Both the dephasing times and the splitting $\Delta\omega/2\pi = 29$ GHz were constant to 20 K. The fact that the pentacene mode retains its identity as a separate and relatively narrow transition indicates that it lies outside the naphthalene vibron band whose $k = 0$ edge is involved in the beating. This confirms the earlier conclusion[25] that this band is well under 1 cm^{-1} in width.

The $t_1 = 0$ phase shift ϕ_b^0 is fit as $2\pi/3$. No simple explanation of this particular value seems possible. The preparation pulses are nearly resonant with electronic transitions for pentacene and nonresonant for naphthalene. In addition, the phases of the relevant dipole matrix elements are not known.

The inset of Fig. 8 shows the frequency distribution of the delayed signal around $\omega_3 = 2\omega_1 - \omega_2$ obtained at fixed delay by scanning the monochromator at high resolution. Although the 1 cm^{-1} splitting between the expected line centers (arrows) is not resolved, it was possible to vary the depth of the beat pattern by setting the monochromator at different points and scanning the delay. This suggests that indeed the signal consists of two contributions unresolved in the short (~6 ps) probe

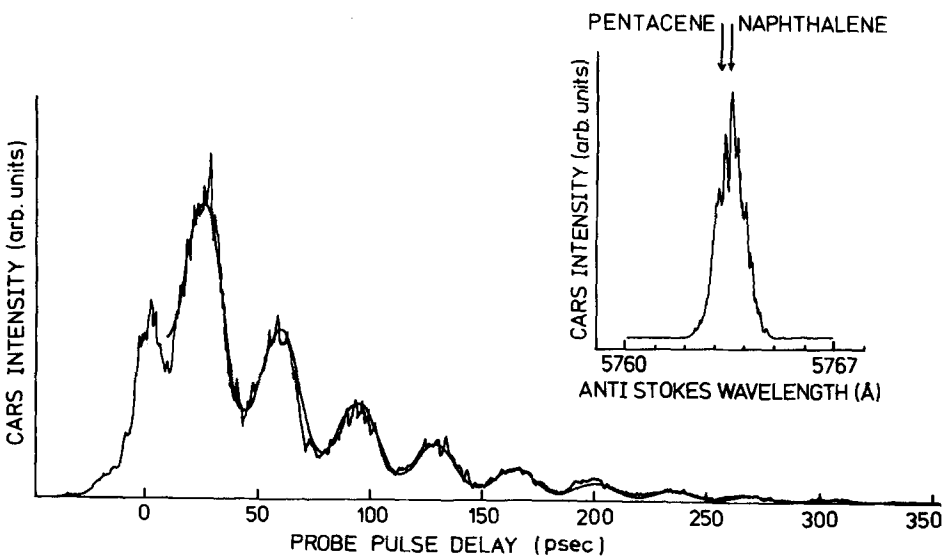

FIG. 8. Interference between the CARS decay of the 767 cm^{-1} vibration of pentacene in naphthalene and the 766 cm^{-1} $k = 0$ states of a naphthalene vibron band. The solid line is a fit to Eq. (5) with beat frequency $\Delta\omega/2\pi = 29$ GHz, zero delay phase shift $\phi^\circ = 120^\circ$, and naphthalene and pentacene phase relaxation times $T_2^n = 156$ ps and $T_2^p = 120$ ps. The inset shows the frequency distribution of the signal around ω_3, taken at a maximum in the CARS decay. The two components indicated by arrows are not well resolved in this dimension due to the short probe pulse.

process, but well resolved during the evolution period of several hundred picoseconds.

III. CONCLUSION

The delayed CARS experiment appears to offer an unambiguous and sensitive method of studying the dephasing of Raman-allowed ground state vibrational transitions even in dilute systems. Enhancement by multiple electronic resonances provides a high degree of selectivity which will be valuable in systems where several sites or several molecular species are present. The rapid advances being made in the power, tunability, repetition rate, and pulse lengths of lasers insure that the technique will become more widely applicable and available. Together with population relaxation studies, this method permits a detailed view of the return of a vibrationally excited guest to equilibrium.

The present results establish the applicability of the method to a number of vibrations and the exponential decays observed justify the analysis of the linewidths in terms of homogeneous broadening mechanisms. The temperature dependent results on the 756 cm^{-1} mode indicate that it is possible for a skeletal vibration to be unaffected by the motion associated with one low frequency mode, but to be sensitive to another. Such situations are known also for C–H and C–D stretches of pure and isotopically mixed crystals of durene.[12–14]

Chemically mixed molecular crystals offer the additional experimental freedom of substantially varying the environment of the observed molecule. Indeed we find differences between the naphthalene and benzoic acid hosts in both the lifetime limited low temperature limit and in the sensitivity of T_2 to temperature. A full understanding of these effects would seem to require the construction of models with the predictive power to relate such results to intermolecular potentials. In the context of such a model, results such as those presented would constitute extremely detailed probes of site structure and motion.

ACKNOWLEDGMENTS

The investigations were supported by the Netherlands Foundation for Chemical Research (S.O.N.) with financial aid from the Netherlands Organization for the Advancement of Pure Research (Z.W.O.).

APPENDIX A

The weak temperature dependence of T_2 for the 756 cm^{-1} mode of pentacene in naphthalene (Sec. IID) contradicts the conclusions of previous work where near-resonant spontaneous Raman scattering of this mode was reported.[34] In both that study, performed with a cw laser, and in a replication of it with 85 ps pulses,[29] two spontaneous emission lines were observed (Fig. 2 of Ref. 34) with irradiation several cm^{-1} to either side of the origin. One line has the inhomogeneous width (e.g., 1.3 cm^{-1} [34]) characteristic of the sample and is centered at $\bar{\omega}_{cb}$, the average of ω_{cb} over the inhomogeneous distribution. The second component is at $\omega_L - 756$ cm^{-1}, following the laser frequency as expected for Raman scattering. The low temperature linewidth for this emission was consistent with that found by time domain CARS (Table I) and is attributable to a value of $2T_1 = 101$ ps. The temperature dependence of this linewidth, when interpreted as $1/\pi c T_2$ [Eq. (1)], was fit to the form of Eq. (4) with $T_2^*(\infty) = 2.4$ ps and $\Delta E/hc = 17$ cm^{-1}. This is inconsistent with the CARS results.

We have now determined that this signal is not Raman scattering from the bulk of the pentacene molecules, which are off resonance by a few cm^{-1}, but is actually spontaneous emission from molecules directly resonant with the incident frequency ω_L. As suggested earlier,[29] an unambiguous distinction can be made by time resolving the emission. This is done by time resolved single photon counting of the dispersed emission with standard techniques while irradiating with 0.2 cm^{-1} (85 ps) pulses 5.5 cm^{-1} to the red or blue of ω_{ca}. The time resolution is 2 ns. The peak at $\omega_L - 756$ cm^{-1} was found to decay to nearly half of its maximum in the 12.5 ns window between pulses. This is consistent with the known fluorescence lifetime of 19.5 ns.[7] It is totally inconsistent with an interpretation of the signal as near-resonant Raman scattering, which would be absent between pulses. The inhomogeneous emission peak at $\bar{\omega}_{cb} = \bar{\omega}_{ca} - 756$ cm^{-1} shows the same time resolved behavior.

It remains to explain why this system shows two fluorescence maxima for a single ground state vibration, why one of them is free from inhomogeneous broadening and tracks the laser frequency, why the preexponential linewidth parameter for this component is twice the value found for the electronic and vibronic transitions studied by photon echoes,[7,8,32] and why no genuine near-resonant Raman scattering is observed.

To answer these questions we need to express the fluorescence intensity as a function of the detected frequency ω and incident frequency ω_L, taking into account the inhomogeneous distributions of electronic and vibronic transition frequencies centered at $\bar{\omega}_{ca}$ and $\bar{\omega}_{cb}$. Let $L_E(\omega - \omega_{cb})$ be the (Lorentzian) probability that a photon of frequency ω is emitted by a molecule in the inhomogeneous distribution having ω_{cb} as the center frequency for its $|c\rangle \rightarrow |b\rangle$ transition. Similarly, let $L_A(\omega_L - \omega_{ca})$ be the cross section for absorption of a laser photon at ω_L by a molecule with its origin centered at ω_{ca}. Let $P(\omega_{ca} - \bar{\omega}_{ca})$ be the inhomogeneous distribution relevant to absorption, i.e., the probability that a molecule has its origin at ω_{ca}. We know that the inhomogeneous distributions around $\bar{\omega}_{ca}$ and $\bar{\omega}_{cb}$ are highly correlated, since, if this were not the case, the CARS observations of Sec. IIC would have shown an inhomogeneous vibrational frequency ω_{ba}. Assume then that the correlation of distributions is perfect. Finally, assume there is no spectral diffusion on the time scale of the fluorescence. With these last two assumptions the probability that a photon absorbed by a transition centered at ω_{ca} is emitted by a transition centered at ω_{cb} is proportional to $\delta(\omega_{ca} - K\omega_{cb})$, where $K = \bar{\omega}_{ca}/\bar{\omega}_{cb}$.

The desired spectrum is the product of these four probabilities integrated over the individual center frequencies ω_{ca} and ω_{cb}:

$$I_f(\omega, \omega_L) = C \int_{-\infty}^{\infty} \int_{-\infty}^{\infty} L_E(\omega - \omega_{cb})\, L_A(\omega_L - \omega_{ca}) \times P(\omega_{ca} - \bar{\omega}_{ca})\, \delta(\omega_{ca} - K\omega_{cb})\, d\omega_{ca} d\omega_{cb} \,. \quad \text{(A1)}$$

The constant C contains all geometric and cross section factors having negligible frequency dependence over the small range of interest. It also includes the incident intensity, which is assumed to be nonsaturating. The laser linewidth and monochromator resolution are assumed in Eq. (A1) to contribute negligibly. At the lower temperatures where these were significant, they were deconvoluted.[34,44] The δ function makes the integral over ω_{ca} trivial giving

$$I_f(\omega, \omega_L) = C \int_{-\infty}^{\infty} L_E(\omega - \omega_{cb})\, L_A(\omega_L - K\omega_{cb}) \times P(K\omega_{cb} - \bar{\omega}_{ca})\, d\omega_{cb} \,. \quad \text{(A2)}$$

Suppose that the distribution P has the constant value p over the region where the product of the other factors in the integrand is significant. Then the emission spectrum is

$$I_f(\omega, \omega_L) = pC \int L_E(\omega - \omega_{cb})\, L_A(\omega_L - K\omega_{cb})\, d\omega_{cb} \quad \text{(A3)}$$

which is the convolution of the homogeneous absorption and emission linewidths. For Lorentzian lines this convolution is also Lorentzian and the observed FWHM is just the sum of contributions from absorption and emission:

$$\nu_{1/2}^{f}(\mathrm{cm}^{-1}) = 1/\pi c T_2^{ac} + 1/\pi c T_2^{bc} \,. \quad \text{(A4)}$$

Each of the two contributions has the form of Eq. (1) with essentially identical T_2^* contributions given by Eq. (2).

The low temperature limits of the two contributions are different. For the absorption process $|c\rangle \leftarrow |a\rangle$, $T_1 = \tau_{fl}$ which contributes a negligible 2.7×10^{-4} cm^{-1} to Eq. (A4). Thus the observed low temperature limit of 0.10 cm^{-1} is due to the T_1 term in the emission process, which is essentially the lifetime of $|b\rangle$.

The situation just described is that of fluorescence line narrowing.[44-46] The emission tracks the laser frequency and the width is given by Eq. (A4) so long as ω_L is in a flat portion of the inhomogeneous distribution. If this picture is applicable it accounts for the position, temperature dependent width, and persistence of the signal after the pulse ends.

What distinguishes this situation from previous examples of fluorescence line narrowing, is that usually the irradiation is at the center of the inhomogeneous distribution. Then $p = P(0)$ in Eq. (A3) and the flatness requirement for P used in passing from Eq. (A2) to Eq. (A3) is simply that the inhomogeneous width is much greater than the homogeneous widths. In the present situation, where the irradiation is up to 9 cm^{-1} from the center of the 1.3 cm^{-1} inhomogeneous origin,[34] a Gaussian $P(\omega_{ca} - \bar{\omega}_{ca})$ would be both rapidly falling [so that Eq. (A3) would not apply] and so small as to make any detectable resonant emission unlikely. We are thus led to suspect that the inhomogeneous distribution is not a simple Gaussian, but rather that the 1.3 cm^{-1} wide part of this distribution observed[34] sits on top of another component, which is at least an order of magnitude broader.

Two additional observations support this view. When a focused beam is used in these experiments, the intensity ratio of the narrowed resonant emission to the inhomogeneously broadened emission from the peak of the distribution is greater when the beam scatters from an imperfection at the front surface than when it passes clearly through the center of the crystal. This leads to the suspicion that the broad component of the inhomogeneous distribution is not uniformly distributed in the crystal volume.

This notion is confirmed by removing the lens before the cryostat so that the crystal is approximately uniformly irradiated. The image of the crystal, magnified to several cm, can then be scanned over the entrance slit of the monochromator. The ratio of the narrow to broad emission is observed to be a factor of 7 greater at an edge of the image than at the center. The crystals are attached at their edges with opaque tape over a 3 mm hole in the copper sample holder. Thus the edges of the image correspond to the visible points nearest to contact with the tape or the copper. The broad inhomogeneity may arise from local strain at these points.

The phenomena described here adequately account for the original observations,[34] but leave open the question of why near-resonant Raman scattering is not observed from the bulk of the pentacene molecules. On the basis of a three level model ($|a\rangle$, $|b\rangle$, $|c\rangle$ of Fig. 1) and continuous irradiation, the Raman scattering should exceed at low temperatures the inhomogeneous fluorescence centered at $\bar{\omega}_{cb}$. This is because there is no pure dephasing to lead to significant population of $|c\rangle$.[5,32,34,44]

The inadequacy of this model may be the neglect of the oscillator strengths of the phonon sideband and the hot transitions from ground manifold phonon states. The absorption spectrum of pentacene in naphthalene[7] shows a largely unresolved phonon sideband with most of its oscillator strength into states which are higher than the fundamental $|c'\rangle$ of the local phonon, but less than ~75 cm^{-1} from the origin. The diffuse contribution to absorption on the blue side leads to fluorescence with little associated Raman scattering, since the phonon lifetimes of the absorbing states will be of the order of $\tau_{c'} = 11$ ps,[7] which is far shorter than the radiative lifetime. In addition the broad hot transition $|c'\rangle \leftarrow |a'\rangle$ is centered ~4 cm^{-1} to the red of the origin[7] and similarly leads to a dominant fluorescence contribution. Finally we note that any broadband background light would lead to fluorescence from $\bar{\omega}_{ca}$ without measurable Raman scattering. The experiment can only be done with those laser frequencies near enough to the origin for signal to be seen, but distant enough that the two emissions are resolved. It is precisely for these frequencies that a three level picture fails to account for all sources of fluorescence excitation and where any genuine Raman is masked by site-selected fluorescence from the broad inhomogeneous component.

[1]F. P. Burke and G. J. Small, J. Chem. Phys. **61**, 4588 (1974).
[2]F. P. Burke and G. J. Small, Chem. Phys. **5**, 198 (1974).
[3]R. M. Hochstrasser and J. E. Wessel, Chem. Phys. **6**, 19 (1974).
[4]K. K. Rabane and P. Saari, J. Lumin. **12/13**, 23 (1976).
[5]R. M. Hochstrasser and C. A. Nyi, J. Chem. Phys. **70**, 1112 (1979).
[6]B. P. Boczar and M. R. Topp, in *Picosecond Phenomena III*, edited by K. B. Eisenthal, R. M. Hochstrasser, W. Kaiser, and A. Laubereau (Springer, Berlin, 1982), p. 174.
[7]W. H. Hesselink and D. A. Wiersma, J. Chem. Phys. **73**, 648 (1980).
[8]W. H. Hesselink and D. A. Wiersma, J. Chem. Phys. **74**, 886 (1981).
[9]H. de Vries and D. A. Wiersma, Phys. Rev. Lett. **36**, 91 (1976).
[10]S. Völker and R. M. Macfarlane, Chem. Phys. Lett. **61**, 421 (1979).
[11]A. I. M. Dicker and S. Völker, Chem. Phys. Lett. **87**, 481 (1982).
[12]C. B. Harris, R. M. Shelby, and P. A. Cornelius, Phys. Rev. Lett. **38**, 1415 (1977).
[13]R. M. Shelby, C. B. Harris, and P. A. Cornelius, J. Chem. Phys. **70**, 34 (1979).
[14]S. Marks, P. A. Cornelius, and C. B. Harris, J. Chem. Phys. **73**, 3069 (1980).
[15]J. C. Bellows and P. N. Prasad, J. Chem. Phys. **70**, 1864 (1979).
[16]L. A. Hess and P. N. Prasad, J. Chem. Phys. **72**, 573 (1980).
[17]P. N. Prasad and R. V. Smith, J. Chem. Phys. **71**, 4646 (1979).
[18]R. A. MacPhail, R. G. Snyder, and H. L. Strauss, J. Chem. Phys. **77**, 1118 (1982).
[19]L. A. Hess and P. N. Prasad, J. Chem. Phys. **78**, 626 (1983).
[20]F. Legay, in *Chemical and Biological Applications of Lasers, Vol. II*, edited by C. B. Moore (Academic, New York, 1977), p. 43.
[21]L. Young and C. B. Moore, J. Chem. Phys. **76**, 5869 (1982).
[22]P. L. Decola, J. R. Andrews, R. M. Hochstrasser, and H. P. Trommsdorff, J. Chem. Phys. **73**, 4695 (1980).
[23]J. R. Andrews and R. M. Hochstrasser, Chem. Phys. Lett. **82**, 381 (1981).
[24](a) J. R. Andrews and R. M. Hochstrasser, Chem. Phys. Lett. **83**, 427 (1981); (b) J. R. Andrews (personal communication, 1983); (c) R. Bozio, P. L. Decola, and R. M. Hochstrasser, in *Time Resolved Vibrational Spectroscopy*, edited by G. H. Atkinson (Academic, New York, 1983); Proceedings of the Lake Placid Conference, August 1982.
[25](a) B. Hesp and D. A. Wiersma, Chem. Phys. Lett. **75**, 423 (1980); (b) D. D. Dlott, C. L. Schosser, and E. L. Chronister, *ibid.* **90**, 386 (1982).
[26]K. Duppen, B. Hesp, and D. A. Wiersma, Chem. Phys. Lett. **79**, 399 (1981).
[27]F. Ho, W.-S. Tsay, J. Trout, and R. M. Hochstrasser, Chem. Phys. Lett. **83**, 5 (1981).
[28]K. Duppen, D. P. Weitekamp, and D. A. Wiersma, in *Picosecond Phenomena III*, edited by K. B. Eisenthal, R. M. Hochstrasser, W. Kaiser, and A. Laubereau (Springer, Berlin, 1982).
[29]D. P. Weitekamp, K. Duppen, and D. A. Wiersma, Phys. Rev. A **27**, 2089 (1982).
[30]D. P. Weitekamp, K. Duppen, and D. A. Wiersma, Chem. Phys. Lett. (accepted for publication).
[31]R. Wertheimer and R. Silbey, J. Chem. Phys. **74**, 686 (1981).
[32]D. A. Wiersma, in *Photoselective Chemistry, Part 2*, edited by J. Jortner (Wiley, New York, 1981), p. 422; W. H. Hesselink and D. A. Wiersma, in *Spectroscopy and Excitation Dynamics of Condensed Molecular Systems*, edited by V. M. Agranovich and R. M. Hochstrasser (North Holland, Amsterdam, 1983), p. 249.
[33]P. de Bree and D. A. Wiersma, J. Chem. Phys. **70**, 790 (1979).
[34]P. de Bree and D. A. Wiersma, Chem. Phys. Lett. **88**, 17 (1982).
[35]F. G. Patterson, H. W. H. Lee, R. W. Olson, and M. D. Fayer, Chem. Phys. Lett. **84**, 59 (1981).
[36]R. W. Olson, H. W. H. Lee, F. G. Patterson, M. D. Fayer, R. M. Shelby, D. P. Burum, and R. M. Macfarlane, J. Chem. Phys. **77**, 2283 (1982).
[37]R. Casalegno and H. P. Trommsdorff, Laser Chem. (to be published).
[38]N. Bloembergen, H. Lotem, and R. T. Lynch, Indian J. Phys. Appl. Phys. **16**, 151 (1978).
[39]K. Duppen, L. W. Molenkamp, J. B. W. Morsink, D. A. Wiersma, and H. P. Trommsdorff, Chem. Phys. Lett. **84**, 421 (1981).
[40]L. W. Molenkamp and D. A. Wiersma, J. Chem. Phys. (submitted).
[41]R. K. Wertheimer, Chem. Phys. **45**, 415 (1980).
[42]R. J. Abbott and D. W. Oxtoby, J. Chem. Phys. **70**, 4703 (1979).
[43]K. Ohno, J. Mol. Spectrosc. **72**, 238 (1978); **77**, 329 (1979).
[44]P. de Bree, dissertation, University of Groningen, 1981.
[45]A. Szabo, Phys. Rev. Lett. **25**, 924 (1970); **27**, 323 (1971).
[46]A. P. Marchetti, W. C. McColgin, and J. H. Eberly, Phys. Rev. Lett. **35**, 387 (1975).